Approximations to solitary waves on lattices, III: the monatomic lattice with second-neighbour interactions

1996 J. Phys. A: Math. Gen. 29 8139

(http://iopscience.iop.org/0305-4470/29/24/035)

J. Phys. A: Math. Gen. **29** (1996) 8139–8157. Printed in the UK

Approximations to solitary waves on lattices, III: the monatomic lattice with second-neighbour interactions

Jonathan A D Wattis

Department of Theoretical Mechanics, University of Nottingham, University Park, Nottingham NG7 2RD, UK

Received 12 August 1996

Abstract. We find new behaviour in a lattice with second-neighbour interactions. First we find solitary waves with oscillatory spatial decay, this is something that cannot occur in lattices with nearest-neighbour interactions alone. This is found by standard asymptotic analysis, which leads to an exact curve in parameter space where this behaviour starts. A number of highly accurate quasi-continuum approximations are derived and solved. One of these suggests a possible method for subsonic solitary waves to cease existing. An alternative method of approximation elegantly reveals the differences in shape between subsonic and supersonic solitary waves. This is based on the weak form of the differential–delay equation for the travelling wave, and is derived using the calculus of variations.

1. Introduction

The subject of solitary waves in lattices with nearest-neighbour interactions has been the topic of many studies [5, 6, 19–21, 26]. Few have studied the effects of adding a second neighbour interaction term. In physical systems this type of interaction would typically be present. Some investigations into its effect have been carried out, by Pnevmatikos *et al* [11, 16, 12, 17] for example. These studies concentrate on numerical simulations after some initial work on continuum expansions. Here we shall concentrate on forming continuum expansions to higher accuracy, and shall see that this can account qualitatively for some of the effects observed numerically in their simulations. For simplicity of algebra, we only consider a harmonic second-neighbour potential energy term. This is obtained from the leading order of a Taylor series of an arbitrary potential, where the second-neighbour interaction is smaller than the nearest-neighbour. We allow the nearest-neighbour interactions to be nonlinear, with a polynomial nonlinearity.

Highly accurate numerical approximations can be generated for the NNI lattice [10], where it has been proven that solitary waves exist [24], but stability of such waves is still unknown, but they are generally assumed to be stable—a view supported by numerical calculations [25]. A similar situation holds in other lattice systems such as the existence of breathers in the discrete sine–Gordon equation which has been proven by MacKay and Aubry [15] and more recently some 'practical' stability results have been derived by Bambusi [1], but a slight modification to the system can dramatically alter the properties [14].

St Pnevmatikos *et al* [16] have studied a more general, diatomic lattice with first- and second-neighbour interactions. They analyse the types of soliton that can travel through the lattice for varying parameter ranges. Diatomic lattices are also mentioned in [17], where the

0305-4470/96/248139+19$19.50

same authors study monatomic and diatomic lattices. They find different types of behaviour for sub- and super-sonic waves.

Some effects of the second-neighbour interaction are known already—the most remarkable is that it allows subsonic travelling waves to exist when the interaction is competitive. These travelling waves are seen to exist in the region just below the speed of sound. At speeds close to zero they appear to be unstable and split into two faster waves, each with smaller amplitude. A mechanism for this was suggested by Flytzanis *et al* [12]. This effect was explained by the use of conservation laws which exist for the continuum limit equation. However, these conservation laws do not hold for the fully discrete equation. We shall supply an alternative mechanism for subsonic waves ceasing to exist as the wave speed is reduced. Our explanation does not contradict the views of Flytzanis *et al*.

For less competitive interactions supersonic solitary waves exist, and for these we find a threshold value where the form of their spatial decay changes from monotone to oscillatory (but still a decay). This threshold is found exactly. The wavelength of the oscillation is analysed, at the onset it is extremely long, but at higher speeds approaches four lattice sites. When the second-neighbour interactions are additive, the effects on the solitary wave form only a quantitative change from the NNI lattice—we find no new behaviour.

The methods used are taken from an earlier work [22], and have been used to explain numerical results from other lattices [23, 27–29]. Despite our approximation of only accounting for harmonic second-neighbour interactions, we expect the results to carry over to anharmonic interactions where the coefficients of nonlinear terms are small: in physical situations the interactions due to second-neighbours will be smaller than those due to nearest-neighbours.

Also a new method outlined in [8] is extended to provide accurate approximations to the shape of solitary waves. This method is based on the variational form of the problem, and provides a simple expression for the waveform, which can distinguish between the shape of subsonic and supersonic solitary waves. This gives a greater intuitive insight than the more complex continuum approximations.

In the remainder of this section we summarize the basic results used in later sections. An important result on the asymptotic form of the tail of a solitary wave is given in section 2. Section 3 is concerned with continuum approximations, and finding good approximations for height, width and overall shape; whilst section 4 uses the method of identities to find a simple, but accurate waveform. Numerical calculations analysing the accuracy of our approximations are included in section 5. A concluding discussion of the results of the paper is contained in section 6.

1.1. Derivation

The kinetic energy is exactly the same as in the usual lattice models, but the potential energy contains an extra term to account for the second-neighbour interactions (W). From these two quantities, we can construct (the Lagrangian and) the Hamiltonian

$$H = \sum_n \tfrac{1}{2} p_n^2 + V(q_{n+1} - q_n) + W(q_{n+2} - q_n). \tag{1.1}$$

Here $V(\cdot)$ is the energy associated with nearest-neighbour interactions, and $W(\cdot)$ is the energy associated with second-neighbour interactions. Hamilton's equations then lead to the 'not-so-intuitive' equation of motion for $\phi_n \equiv q_{n+1} - q_n$

$$\begin{aligned}\ddot{\phi}_n = {} & V'(\phi_{n+1}) - 2V'(\phi_n) + V'(\phi_{n-1}) + W'(\phi_{n+2} + \phi_{n+1}) - W'(\phi_{n+1} + \phi_n) \\ & - W'(\phi_n + \phi_{n-1}) + W'(\phi_{n-1} + \phi_{n-2}).\end{aligned}$$

It has already been mentioned that second-neighbour interactions (SNI) are weaker than nearest-neighbour interactions (NNI); to this end we shall only consider the harmonic part of SNI; i.e. $W(\theta) = \frac{1}{2}g\theta^2$. Whereupon the equation of motion simplifies to

$$\ddot{\phi}_n = V'(\phi_{n+1}) - 2V'(\phi_n) + V'(\phi_{n-1}) + g(\phi_{n+2} - 2\phi_n + \phi_{n-2}). \tag{1.2}$$

We assume a polynomial model for V, $V'(\phi) = \phi + a\phi^2 + b\phi^3$, following [10, 17].

If we make the travelling wave ansatz, $\phi_n(t) = \phi(n - ct) = \phi(z)$, we obtain an equation with a single independent variable

$$c^2\phi''(z) = V'(\phi(z+1)) - 2V'(\phi(z)) + V'(\phi(z-1)) + g[\phi(z+2) - 2\phi(z) + \phi(z-2)] \tag{1.3}$$

and it is this differential–delay–advance equation that we shall put our efforts to.

1.2. Dispersion relation

We linearize the equation of motion around the zero solution ($\phi = 0$), and substitute a linear wave solution ($\phi = \exp \mathrm{i}(kn - \omega t)$)

$$\omega^2(k) = 4\sin^2(\tfrac{1}{2}k) + 4g\sin^2(k) \qquad c^2(k) = 4\frac{\sin^2(\frac{1}{2}k)}{k^2} + 4g\frac{\sin^2(k)}{k^2}.$$

The speed of sound in the lattice is then, $c_0 = \sqrt{1+4g}$, and we have the condition that $g > -\frac{1}{4}$ for the propagation of small disturbances. If $g < -\frac{1}{4}$, c_0 will be imaginary and we have solutions of the form $\phi = \exp(\gamma t + \mathrm{i}kn)$ with $\gamma \in \mathbb{R}$. This indicates that the zero solution is unstable if the second-neighbour interactions are competitive and strong enough.

1.3. Standard continuum approximation

Using the standard arguments of forming a continuum approximation, one assumes ϕ to be a small and slowly varying function of the continuous variables (x, t). We keep second derivatives of all terms, and fourth derivatives only of linear terms, to end up with a soluble equation

$$\phi_{tt} = (V'(\phi))_{xx} + 4g\phi_{xx} + \tfrac{1}{12}\phi_{xxxx} + \tfrac{4}{3}g\phi_{xxxx} + \mathcal{O}(\phi_{xxxxxx}, (\phi^p)_{xxxx}). \tag{1.4}$$

The travelling wave solution $\phi(z) = \phi(x - ct)$ then satisfies $c^2\phi = V'(\phi) + 4g\phi + \frac{1}{12}(1 + 16g)\phi''$ which can be integrated once further to

$$\tfrac{1}{24}(1+16g)\phi'^2 = \tfrac{1}{2}(c^2 - 4g - 1)\phi^2 - \frac{a}{p+1}\phi^{p+1} \tag{1.5}$$

so, we can see that solutions will exist with $c^2 < 1 + 4g$ provided that $g < -\frac{1}{16}$. The speed of sound in the lattice is seen, from the dispersion relation, to be $\sqrt{1+4g}$, so that these solutions correspond to subsonic solitons, and are an effect of second-neighbour interactions. If $g > -\frac{1}{16}$, then supersonic solitons exist (as in the purely NNI lattices). We cannot have both supersonic and subsonic solitons existing in a single system.

The continuum solution for sub- and supersonic solitary waves in the cubic lattice is

$$\phi_{\mathrm{cub}}(z) = \frac{3}{2a}(c^2 - 4g - 1)\operatorname{sech}^2\left(z\sqrt{\frac{3(c^2-4g-1)}{1+16g}}\right) \tag{1.6}$$

and for the quartic lattice

$$\phi_{\mathrm{qu}}(z) = \sqrt{\frac{2}{b}(c^2 - 4g - 1)}\operatorname{sech}\left(2z\sqrt{\frac{3(c^2-4g-1)}{1+16g}}\right). \tag{1.7}$$

The half-height widths of these waves are

$$\begin{aligned}\text{width}_{\text{cub}} &= 2\sqrt{\frac{1+16g}{3(c^2-4g-1)}}\,\log(1+\sqrt{2})\\ \text{width}_{\text{qu}} &= \sqrt{\frac{1+16g}{3(c^2-4g-1)}}\,\log(2+\sqrt{3}).\end{aligned} \tag{1.8}$$

The energy carried by the soliton can also be approximated, by $\phi(z) = q(z+1) - q(z) \simeq q'(z)$ and $\frac{\mathrm{d}}{\mathrm{d}t}(q) = -c\frac{\mathrm{d}}{\mathrm{d}z}(q) \simeq -c\phi(z)$ thus,

$$H = \int_{-\infty}^{\infty} \tfrac{1}{2}c^2\phi(z)^2 + V(\phi(z)) + \tfrac{1}{2}g[\phi(z+1)+\phi(z)]^2\,\mathrm{d}z. \tag{1.9}$$

For the cubic and quartic lattices, this expression can be calculated exactly. The results are

$$\begin{aligned}H_{\text{cub}} &= \frac{1}{10a^2}(c^2-4g-1)\sqrt{3(1+16g)(c^2-4g-1)}\\ &\qquad\times\left[9c^2+1-6g+30g\left(\frac{\beta\cosh\beta-\sinh\beta}{\sinh^3\beta}\right)\right]\\ H_{\text{qu}} &= \frac{1}{3b\sqrt{3}}\sqrt{(c^2-4g-1)(1+16g)}[5c^2+1-2g+12g\beta\,\text{csch}(2\beta)]\\ \beta &= \sqrt{\frac{3(c^2-4g-1)}{(1+16g)}}.\end{aligned} \tag{1.10}$$

These expressions give reasonable results for c^2 close to $1+4g$, where $H_{\text{cub}} \sim (c^2-4g-1)^{3/2}$ and $H_{\text{qu}} \sim (c^2-4g-1)^{1/2}$. These are two quite different types of behaviour. The expressions given here are valid for both subsonic and supersonic waves, whichever is appropriate according to the value of g. The high speed limits vary with $H_{\text{cub}} \sim c^4$ and $H_{\text{qu}} \sim c^3$ as $c \to \infty$.

In both cases subsonic solitons exist on the sublinear side of the nonlinear potential gradient, hence for it to exist in a quartic lattice the coefficient of nonlinearity must be negative ($b < 0$). Supersonic solitons exist on the superlinear side of the potential gradient.

This is only a continuum approximation, and in the limit $c \to \infty$, this formula predicts that the waves will become arbitrarily narrow. The lattice structure however, will not allow this, and in such a region of parameter space, another approximation method is needed. Such approximations will be derived in sections 3 and 4.

2. Asymptotics

If we examine how the soliton decays, we find new behaviour not found in simpler models. Assuming the decay of ϕ is given by $\phi(z) \sim \exp(-\lambda z) + \text{cc}$ with λ possibly complex, we find

$$c^2 = \frac{2(\cosh(\lambda)-1)}{\lambda^2} + \frac{2g(\cosh(2\lambda)-1)}{\lambda^2} \stackrel{\text{def}}{=} R(\lambda). \tag{2.1}$$

Now we examine the function $R(\lambda)$. For $g > 0$ the function is positive and increases without bound. Thus, there is a $\lambda \in \mathbb{R}$ for each $c > 1+4g$. However, for $-\frac{1}{16} < g < 0$, $R(\lambda)$ has a maximum value R_{M}, and for speeds above $\sqrt{R_{\text{M}}}$ no monotone decay is possible. Thus these fast waves in a lattice with competitive SNI have oscillatory decay. For $-\frac{1}{4} < g < -\frac{1}{16}$ we have only subsonic solitons so that large speeds are not allowed. The new, interesting

case is then fast waves with $-\frac{1}{16} < g < 0$, and we aim to find the onset point of oscillatory decay.

Defining $\bar{\lambda}$ by $R'(\bar{\lambda}) = 0$, we can find the curve in a c–g plane where oscillatory decay starts. It is given parametrically by $\bar{\lambda}$

$$g = \frac{-(\bar{\lambda} - 2\tanh(\frac{1}{2}\bar{\lambda}))}{4(\bar{\lambda}\cosh\bar{\lambda} - \sinh\bar{\lambda})} \qquad c = \sqrt{R(\bar{\lambda})}. \tag{2.2}$$

From these formulae, we can find two limits, as $\bar{\lambda} \to 0$, $g \to -\frac{1}{16}$ and $c \to \sqrt{1+4g}$, this is the continuum approximation, with low flat solitary waves travelling close to the speed of sound in the lattice. The other limit, $\bar{\lambda} \to \infty$ has $c \to \infty$ and $g \to 0$. For $\lambda \in \mathbb{C}$, we put $\lambda = \mu + \mathrm{i}\nu$, $\mu, \nu \in \mathbb{R}$. By writing down the real and imaginary components of (2.1) we can see that when the decay is oscillatory, we still have $\mu > 0$ and so the amplitude continues to decay.

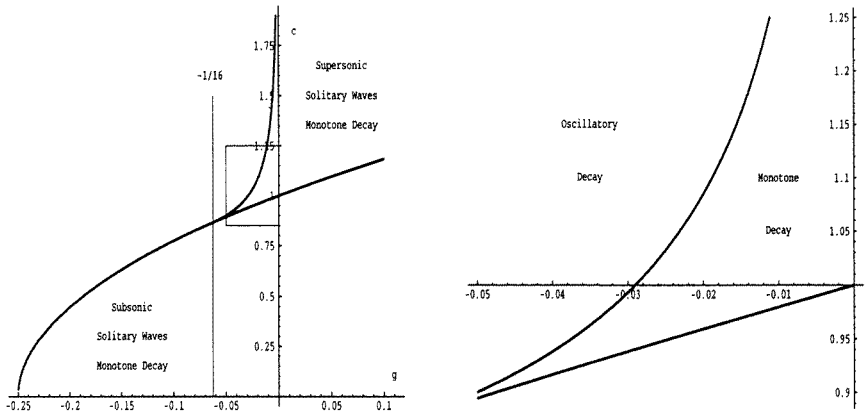

Figure 1. The figure shows the types of behaviour that are found in the c–g parameter space; with an enlargement of the boxed region.

To gain more idea of the behaviour of this oscillation we can investigate a limit using further asymptotics. The bifurcation from $\nu = 0$ is continuous so that near the bifurcation, ν will be small and the oscillations have large wavelengths. However, away from the bifurcation point it is not so clear what will happen. It can be shown that as $\mu \to \infty$, ν tends to $\pi/2$ and $c \to \infty$. Thus, the spatial decay of the wave continues to strengthen as the speed increases. To be more specific

$$\nu \sim \tfrac{1}{2}\pi(1 - \mu^{-1}) \qquad \text{as } \mu \to \infty \tag{2.3}$$

and $c \sim \mu^{-1}e^{\mu}\sqrt{-g}$. This corresponds to the oscillation having a wavelength of four particles (the amplitude decay, however, means that no part of the soliton is actually periodic). This conclusion is reached by a process of elimination, ν can never equal $n\pi/2$, whatever values c, μ take. Thus, $\pi/2$ is the only consistent limit for ν.

This has important implications for the interpretation of numerical simulations. The presence of ripples in a soliton tail need not imply the non-existence of a solitary wave. Simulations which start with an approximation to a solitary wave and wait for the time evolution to separate out an exact solitary wave from the radiation (using the ideas of the IST from integrable systems) cannot be used to claim non-existence simply due to the development of ripples.

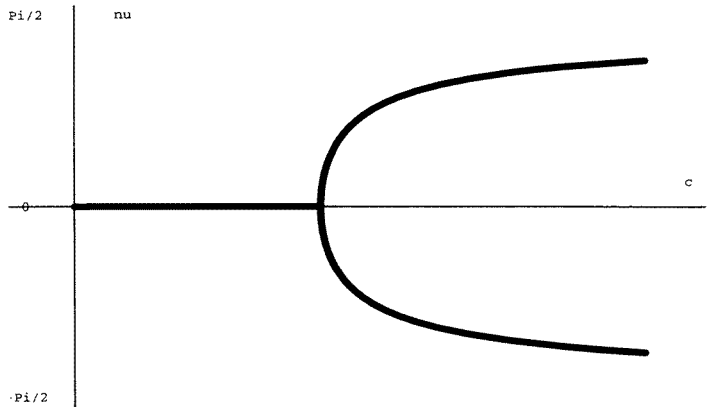

Figure 2. The figure shows how the imaginary part of the exponent varies with speed in the range $g \in (-\frac{1}{16}, 0)$.

3. Continuum approximations

We shall formulate the approximations in Fourier space, where the operator is a function of the transform variable k. From the equation for the travelling wave (1.3), we put $F(z) = V'(\phi(z))$ and denote Fourier transforms by $\hat{\phi}(k)$, $\hat{F}(k)$.

Taking the Fourier transform of equation (1.3)

$$c^2k^2\hat{\phi}(k) = 4\hat{F}(k)\sin^2(\tfrac{1}{2}k) + 4g\hat{\phi}(k)\sin^2(k). \tag{3.1}$$

Continuum approximations are formed by expanding around a solution dominated by long wave modes, i.e. $\hat{\phi}(k)$ is dominated by its small k component. Hence it is important for the operator to be accurately approximated near $k = 0$. We first isolate the operator, that is all terms explicitly involving k, into a single multiplier, which we shall denote $\hat{\Lambda}(k)$.

$$\hat{\Lambda}(k)\hat{\phi}(k) = \left(\frac{c^2k^2 - 4g\sin^2(k)}{4\sin^2(\frac{1}{2}k)}\right)\hat{\phi}(k) = \hat{F}(k). \tag{3.2}$$

Padé approximates of the operator $\hat{\Lambda}(k)$ are now formed by expanding around $k = 0$ to obtain various equations. On inverting the transform, quadratic terms in k become second-derivative operators, and we are left with an autonomous second-order ODE which approximates the differential–delay equation. In all cases a solution is achievable, but some require much algebra. This is in contrast to the differential–delay equation, to which there are no known solutions. An approximate speed–height relationship is easily derivable, and will be quoted.

3.1. (2, 0) *Padé approximation*

The method of approximation used in this section follows the ideas of Rosenau [19] and leads to generalizations of the equations originally found by Collins [5] and Collins and Rice [6]. Here we approximate $\hat{\Lambda}(k)$ by the (2,0) Padé approximate $(c^2 - 4g) + \frac{1}{12}(c^2 + 12g)k^2$, and upon inverting the Fourier transform, the ODE we have to solve is (from 3.2)

$$(c^2 - 4g)\phi - \tfrac{1}{12}(c^2 + 12g)\phi'' = V'(\phi) \tag{3.3}$$

which in the cases of cubic or quartic potentials, can be completely solved

$$\phi_{\rm cub}(z) = \frac{3}{2a}(c^2 - 4g - 1)\,\mathrm{sech}^2\left(z\sqrt{\frac{3(c^2-4g-1)}{(c^2+12g)}}\right)$$
$$\phi_{\rm qu}(z) = \sqrt{\frac{2}{b}(c^2 - 4g - 1)}\,\mathrm{sech}\left(2z\sqrt{\frac{3(c^2-4g-1)}{(c^2+12g)}}\right).$$

Note we obtain the same speed–height scaling as in the standard continuum approximation, but we find a new, non-singular width scale—that is as we increase the speed (c), the width tends to a finite constant. The half-height widths are given by,

$$\mathrm{width}_{\rm cub} = 2\sqrt{\frac{(c^2+12g)}{3(c^2-4g-1)}}\log(1+\sqrt{2}) \qquad \mathrm{width}_{\rm qu} = \sqrt{\frac{(c^2+12g)}{3(c^2-4g-1)}}\log(2+\sqrt{3}).$$

Using a more accurate expression for the waveform, we can also find a better estimate of the energy carried by the wave. The expansion

$$\phi(z) = q(z+\tfrac{1}{2}) - q(z-\tfrac{1}{2}) \simeq q'(z) + \tfrac{1}{24}q'''(z) \tag{3.4}$$

can be inverted to find $q'(z) \simeq \phi - \frac{1}{24}\phi''$. Thus an improved expression for the kinetic energy is found, leading to a formula for the total energy which is more accurate than (1.9).

$$H = \int_{-\infty}^{\infty} \tfrac{1}{2}c^2\phi(z)^2 + \tfrac{1}{24}c^2\phi'(z)^2 + V(\phi(z)) + \tfrac{1}{2}g[\phi(z+1)+\phi(z)]^2\,\mathrm{d}z. \tag{3.5}$$

Explicitly

$$\begin{aligned} H_{\rm cub} &= \frac{(c^2-4g-1)^{3/2}}{10a^2}\sqrt{3(c^2+12g)} \\ &\quad\times\left[9c^2 + 1 - 6g + \frac{1}{3}c^2\beta^2 + 30g\left(\frac{\beta\cosh\beta - \sinh\beta}{\sinh^3\beta}\right)\right] \\ H_{\rm qu} &= \frac{1}{3b\sqrt{3}}\sqrt{(c^2-4g-1)(c^2+12g)}[5c^2 - 2g + 4 + \tfrac{1}{3}\beta^2 + 4g\beta\,\mathrm{csch}(2\beta)] \\ \beta &= \sqrt{\frac{3(c^2-4g-1)}{(c^2+12g)}}. \end{aligned} \tag{3.6}$$

The behaviour of the energy near the speed of sound is unchanged, both lattices have zero energy at this point (since the soliton formally has zero amplitude here). The large speed asymptotics is modified, $H_{\rm cub} \sim c^6$ and $H_{\rm qu} \sim c^4$ as $c \to \infty$.

3.2. (0, 2) *Padé approximation*

This case is one of the more complex approximations, since we have the differential operator acting upon the nonlinear term

$$(c^2 - 4g)\phi(z) = \left[1 + \frac{(c^2+12g)}{12(c^2-4g)}\left(\frac{\mathrm{d}}{\mathrm{d}z}\right)^2\right]V'(\phi(z)). \tag{3.7}$$

If we were to ignore the derivatives of nonlinear terms, the standard continuum approximation would be recovered. Since we keep this term, we expect to get a more

accurate approximation. Keeping this extra term, the equation can still be integrated; first to

$$12(c^2-4g)^2[\phi V'(\phi)-V(\phi)] = 6(c^2-4g)V'(\phi)^2 + \tfrac{1}{2}(c^2+12g)\phi'^2 V''(\phi)^2. \tag{3.8}$$

The constant of integration is zero since we have quiescent boundary conditions as $z \to \pm\infty$. For a speed-height relation we put $\phi'(z) = 0$. To obtain the height (ϕ_0) as a function of speed (c) requires the solution of a quadratic; we keep both possible roots for the time being, and use the upper sign to denote the root which matches with the continuum approximation result in the limit of small height.

$$\begin{aligned} a\phi_{0,\mathrm{cub}} &= \tfrac{2}{3}(c^2-4g) - 1 \pm \tfrac{1}{3}\sqrt{(c^2-4g)(4c^2-16g-3)} \\ b\phi_{0,\mathrm{qu}}^2 &= \tfrac{3}{4}(c^2-4g) - 1 \pm \tfrac{1}{4}\sqrt{(c^2-4g)(9c^2-36g-8)}. \end{aligned} \tag{3.9}$$

We now consider the equations (3.9) as bifurcation curves in (c, ϕ_0) space. For certain parameter values, these curves consist of a single connected line which bends back on itself. Thus, the approximations (3.9) open up the possibility of a saddle-node bifurcation occurring in parameter space (see figure 4). The methods that generate this result rely on an approximation around $c = \sqrt{(1+4g)}$, $\phi(z) \approx 0$ and so cannot be expected to give rigorous results near a bifurcation point. It would be interesting to see the results of a numerical path-following investigation of this problem. All the approximation methods above predict a branch which extends all the way back to $c = 0$, however, the numerics of Flytzanis *et al* [12] suggest that as the speed is reduced, the branch of subsonic solitons either becomes unstable (with the possibility of an associated bifurcation) or ceases to exist.

To find the shape of the waveform that this approximation generates, we take the differential equation (3.8), separate and integrate to find

$$z(\phi) = \pm\sqrt{\frac{c^2+12g}{12(c^2-4g)}}\left[4\tan^{-1}\sqrt{\frac{\phi_0-\phi}{\phi-\bar{\phi}_0}} - \frac{2}{a\bar{\phi}_0}\sqrt{\frac{-\bar{\phi}_0}{\phi_0}}\tanh^{-1}\left(\sqrt{\frac{\bar{\phi}_0}{\phi_0}}\sqrt{\frac{\phi_0-\phi}{\phi-\bar{\phi}_0}}\right)\right] \tag{3.10}$$

in the case of supersonic waves in the cubic lattice ($g > -\frac{1}{16}$, $c^2 > 1+4g$); and

$$z(\phi) = \pm\sqrt{\frac{c^2+12g}{12(c^2-4g)}}\left[4\tan^{-1}\sqrt{\frac{\phi_0-\phi}{\phi-\bar{\phi}_0}} - \frac{2}{a\bar{\phi}_0}\sqrt{\frac{-\bar{\phi}_0}{\phi_0}}\tan^{-1}\left(\sqrt{\frac{\bar{\phi}_0}{\phi_0}}\sqrt{\frac{\phi_0-\phi}{\phi-\bar{\phi}_0}}\right)\right] \tag{3.11}$$

in the case of subsonic waves in the cubic lattice ($-\frac{1}{4} < g < -\frac{1}{16}$, $c^2 < 1+4g$). In each case, the implicit expression can be converted to a equation which is easily solved numerically. A simple way of accomplishing this is by substituting $\Theta = \sqrt{(\phi_0-\phi)/(\phi-\bar{\phi}_0)}$, solving the equation for Θ, then finding ϕ from Θ. The momentum can then be obtained from a rearrangement of the differential equation (3.8). A similar procedure can be carried out for the quartic lattice.

3.3. (2, 2) *Padé approximation*

This approximation gains an extra order of accuracy over the methods described so far. By allowing a differential operator to act on both sides of the equation, an extra term in the Taylor series of $\hat{\Lambda}(k)$ can be accommodated. All the above approximations have dealt with terms which arise from fourth spatial derivatives in a PDE approximation of the lattice. This approximation also effectively accommodates the sixth spatial derivatives, but by using a

Padé approximation, no higher derivatives actually appear in our equations. Instead we pay for the extra accuracy in more cumbersome algebra—the terms we do have to deal with become more complicated. We write the operator as

$$\hat{\Lambda}(k) \sim \frac{\alpha - \beta k^2}{1 - \gamma k^2} \qquad \alpha = (c^2 - 4g)$$
$$\beta = \frac{-(c^4 + 96c^2 g + 240g^2)}{30(c^2 + 12g)} \qquad \gamma = \frac{(c^2 - 20g)}{20(c^2 + 12g)}. \tag{3.12}$$

Whereupon the differential equation $[\alpha + \beta(\frac{\mathrm{d}}{\mathrm{d}z})^2]\phi = [1 + \gamma(\frac{\mathrm{d}}{\mathrm{d}z})^2]V'(\phi)$ integrates to

$$2(\beta - \alpha\gamma)V(\phi) + 2\alpha\gamma\phi V'(\phi) - \gamma V'(\phi)^2 - \alpha\beta\phi^2 = \phi'(z)^2[\gamma V''(\phi) - \beta]^2. \tag{3.13}$$

The speed–height relation is easily obtained from this first integral

$$a\phi_0^{p-1} = (c^2 - 4g - 1) - \frac{5(c^2 + 12g)^2}{3(p+1)(c^2 - 20g)} \times \left[1 \mp \sqrt{1 + \frac{3(p^2-1)(c^2 - 20g)(c^2 - 4g - 1)}{5(c^2 + 12g)^2}}\right]. \tag{3.14}$$

This formula has two branches of solutions, as the $(0, 2)$ Padé approximation also had. Again the upper sign gives the root which agrees with the simpler approximations near the speed of sound. The two curves (3.14) can be considered as branches in bifurcation space with parameter c^2. Unfortunately, in this case the two curves do not meet at a point where c^2 is positive (so we do not actually see the bifurcation point). This is disappointing, but since these methods are based on an expansion around the point $c^2 = 1 + 4g$, $\phi = 0$, we only expect quantitatively accurate results near this point, and not at points far away from this. The waveform from this approximation can be found in a similar way to the method outlined for the $(0, 2)$ Padé approximation.

3.4. Global approximation of operator

All the above methods predict that at high speeds the solitary waves become narrow (with their widths being of the order of the lattice spacing), and so their Fourier transforms will be expected to contain a high k component. Yet the earlier approximations all rely on expansions around $k = 0$. To form accurate approximations in the large speed (c) parameter range, we need an approximation of the operator which will take account of the high frequency component as well as the low.

Hence, we suggest an approximation of the form $\hat{\lambda} = [\alpha + \beta k^2]$. By considering the values of each operator at $k = 0$ and $k \to \infty$ we deduce that $c^2 - 4g$ and $\frac{1}{2}c^2$ are suitable values for α, β respectively. The solution of the equation $[\alpha + \beta k^2]\hat{\phi} = \hat{F}$ is obtained by inverting the Fourier transform and solving the ODE, $\alpha\phi - \beta\phi'' = V'(\phi)$. The solutions are then

$$\phi_{\mathrm{cub}}(z) = \frac{3}{2a}(c^2 - 4g - 1)\,\mathrm{sech}^2\left(\frac{z}{c}\sqrt{\tfrac{1}{2}(c^2 - 4g - 1)}\right)$$
$$\phi_{\mathrm{qu}}(z) = \sqrt{\frac{2}{b}(c^2 - 4g - 1)}\,\mathrm{sech}\left(\frac{z}{c}\sqrt{2(c^2 - 4g - 1)}\right)$$

for the cubic and quartic potentials respectively. The widths of these waves are:

$$\begin{aligned}\text{width}_{\text{cub}} &= \frac{2c\sqrt{2}\log(1+\sqrt{2})}{\sqrt{c^2-4g-1}} \longrightarrow 2\sqrt{2}\log(1+\sqrt{2}) \approx 2.49\\ \text{width}_{\text{qu}} &= \frac{c\sqrt{2}\log(2+\sqrt{3})}{\sqrt{c^2-4g-1}} \longrightarrow \sqrt{2}\log(2+\sqrt{3}) \approx 1.86.\end{aligned} \tag{3.15}$$

Note that this method is not applicable in the subsonic range (where $c^2 - 4g - 1 < 0$).

4. Method of identities

In this section, we generalize the results of [8] to the lattice with second-neighbour interactions, and give an explanation of the reasons why this method works. It is based on the variational form of the equations.

The identities are obtained by multiplying the travelling wave equation (1.3 through by a test function $\psi(z)$, and integrating over the entire range of z $(-\infty, \infty)$. This is similar to the method used when seeking weak solutions of an equation. After integration by parts, the general identity

$$\begin{aligned}\int c^2\phi(z)\psi''(z)\,\mathrm{d}z = &\int V'(\phi(z))[\psi(z+1) - 2\psi(z) + \psi(z-1)]\,\mathrm{d}z\\ &+ \int g\phi(z)[\psi(z+2) - 2\psi(z) + \psi(z-2)]\,\mathrm{d}z.\end{aligned} \tag{4.1}$$

is obtained [8]. We assume that the waveform $\phi(z)$ is an even function. Then if $\psi(z)$ is odd, all the integrals collapse to zero, and we are left with no information to determine ϕ; the test function $\psi(z) = 1$ also gives trivial results. So the test functions we use are the first three even polynomials, $\psi(z) = \frac{1}{2}z^2, \frac{1}{2}z^4, \frac{1}{2}z^6$, which generate the three identities

$$\begin{aligned}c^2\int \phi(z)\,\mathrm{d}z &= \int V'(\phi(z))\,\mathrm{d}z + 4g\int \phi(z)\,\mathrm{d}z\\ 6c^2\int z^2\phi(z)\,\mathrm{d}z &= \int (6z^2+1)V'(\phi(z))\,\mathrm{d}z + 4g\int (6z^2+4)\phi(z)\,\mathrm{d}z\\ 15c^2\int z^4\phi(z)\,\mathrm{d}z &= \int (15z^4+15z^2+1)V'(\phi(z))\,\mathrm{d}z\\ &\quad + 4g\int (15z^4+60z^2+16)\phi(z)\,\mathrm{d}z.\end{aligned} \tag{4.2}$$

Following the comments made earlier, we try an ansatz function that is even, decays exponentially at infinity, and has free parameters that can be fitted using the identities. We consider the three parameter fit, $\phi(z) = A\,\mathrm{sech}^n(\beta z)$. The half-height-width of such a wave is given by

$$\text{width} = \frac{2}{\beta}\log\left(2^{1/n} + \sqrt{2^{2/n}-1}\right) \tag{4.3}$$

which remains finite in both $n \to 0, \infty$ limits.

The first identity fits the height (A) with some dependence on n; the second, a width scale (β)

$$A^{p-1} = \frac{I_{0,n}}{I_{0,np}}\left(\frac{c^2-4g-1}{a}\right) \qquad \beta^2 = 6\left(\frac{c^2-4g-1}{c^2+12g}\right)\left(\frac{I_{2,n}}{I_{0,n}} - \frac{I_{2,np}}{I_{0,np}}\right). \tag{4.4}$$

Here the quantity $I_{m,n}$ is defined by

$$I_{m,n} = \int_{-\infty}^{\infty} x^m \operatorname{sech}^n(x)\,\mathrm{d}x. \tag{4.5}$$

The third identity is used to fix n—a 'shape' parameter. To obtain anything useful from this, involves long and tedious algebra. The final result is a quadratic in c^2 where the coefficients are complicated functions of n. This can be solved to give speed as a function of n and then also plot height, and width as parametric functions of n. (See the appendix for further details of this calculation.) The results suggest that for subsonic waves, n takes values less than 2, (the continuum limit value), but stops short of n falling to zero.

As n increases from its continuum value, ($n = 2$ for the cubic lattice and $n = 1$ for the quartic lattice), the method of identities provides a fit for supersonic waves which exceeds the accuracy of the standard continuum approximation. The limit $n \to \infty$ gives a positive bounded value for c_∞ provided $g \gtrsim -0.01$ and bounded, to be precise

$$c_\infty^2 = 3 + 132g + \sqrt{9 + 912g + 17\,664g^2}. \tag{4.6}$$

This limit corresponds to using a Gaussian pulse (formed from $\lim_{n\to\infty} \operatorname{sech}^n(x/\sqrt{n})$). In the case of a NNI lattice this type of pulse was seen to be a good fit for a wide range of speeds [8]. Here, we find similar results. The form is given more completely by

$$\phi(z) = \left(\frac{\sqrt{p}(c^2 - 4g - 1)}{a}\right)^{1/(p-1)} \exp\left(-3z^2\left(\frac{p-1}{p}\right)\left(\frac{c^2 - 4g - 1}{c^2 + 12g}\right)\right) \tag{4.7}$$

where only the first two identities can be satisfied, since there are only two parameters (height and width—there is now no shape parameter to take the place of n). For any speed above c_∞, this approximation is more accurate than any corresponding $A\operatorname{sech}^n(\beta z)$ formula for finite n with coefficients given by (4.4).

4.1. Derivation of identities from Lagrangian

As already stated, the system we are considering is a Hamiltonian and Lagrangian system. Whilst the Hamiltonian is widely known to be the energy, an interpretation of the Lagrangian is not so accessible [31]. The identities described earlier were derived in a very simple way, directly from the equation for the travelling wave (1.3). Here, we shall demonstrate that these identities are in fact a consequence of the Lagrangian structure. Our Lagrangian is

$$L = \sum_n \tfrac{1}{2}\dot{q}_n^2 - V(q_{n+1} - q_n) - W(q_{n+2} - q_n). \tag{4.8}$$

The equations of motion are derived by setting the first variation of the time integral to zero ($\delta \int L\,\mathrm{d}t = 0$). Thus, scaling L by a constant does not alter the equations of motion. We now impose the travelling wave ansatz into the Lagrangian, integrate from $t = 0$ to $t = 1/c$ and rescale to obtain

$$\mathcal{S}[q] = \int_{z\in\mathbb{R}} \tfrac{1}{2}c^2 q'(z)^2 - V(q(z+1) - q(z)) - W(q(z+2) - q(z))\,\mathrm{d}z \tag{4.9}$$

where q is a function of $z \stackrel{\text{def}}{=} n - ct$.

We now examine critical points of this functional. Let $\tilde{q}(z)$ be a critical point of the integral, $r(z)$ an arbitrary perturbation with unit norm, and $\epsilon \ll 1$ a small parameter. The first variation is defined as a Gateaux derivative

$$\delta\mathcal{S}[q]r = \lim_{\epsilon\to 0} \frac{\mathcal{S}[q + \epsilon r] - \mathcal{S}[q]}{\epsilon}. \tag{4.10}$$

A turning point for $\mathcal{S}$ is sought, i.e. a function $\tilde{q}(z)$ such that $\delta\mathcal{S}[\tilde{q}]r = 0$ for any $r(z)$. One such condition is

$$\int r(z)[c^2\tilde{q}''(z) - V'(\tilde{q}(z+1) - \tilde{q}(z)) + V'(\tilde{q}(z) - \tilde{q}(z-1)) \\ -W'(\tilde{q}(z+2) - \tilde{q}(z)) + W'(\tilde{q}(z) - \tilde{q}(z-2))]\,\mathrm{d}z = 0. \tag{4.11}$$

Since this integral must vanish for all functions $r(z)$, the term in square brackets must equal zero, which gives the travelling wave equation (1.3). Alternatively, we can write this integral in a weak form, using integration by parts to remove the derivatives from $\tilde{q}''(z)$ and place them on $r(z)$ instead.

$$\int c^2\tilde{q}(z)r''(z) + [r(z+1) - r(z)]V'[\tilde{q}(z+1) - \tilde{q}(z)] \\ +[r(z+2) - r(z)]W'[\tilde{q}(z+2) - \tilde{q}(z)]\,\mathrm{d}z = 0. \tag{4.12}$$

We define the variable $\phi(z) = \tilde{q}(z+1) - \tilde{q}(z)$, and eliminate $\tilde{q}$ which describes a kink, in favour of $\phi(z)$ which has the form of a pulse. A second equation is obtained by changing variables, $z \mapsto z+1$ (in 4.12) and subtracting the two equations to express the result purely in terms of $\phi(z)$. The final result is then

$$c^2\int r''(z)\phi(z)\,\mathrm{d}z = \int [r(z+1) - 2r(z) + r(z-1)]V'[\phi(z)]\,\mathrm{d}z \\ + \int [r(z+2) - r(z+1) - r(z) + r(z-1)]W'[\phi(z) + \phi(z+1)]\,\mathrm{d}z \tag{4.13}$$

which in the case of harmonic $W(\cdot)$ reduces to equation (4.1).

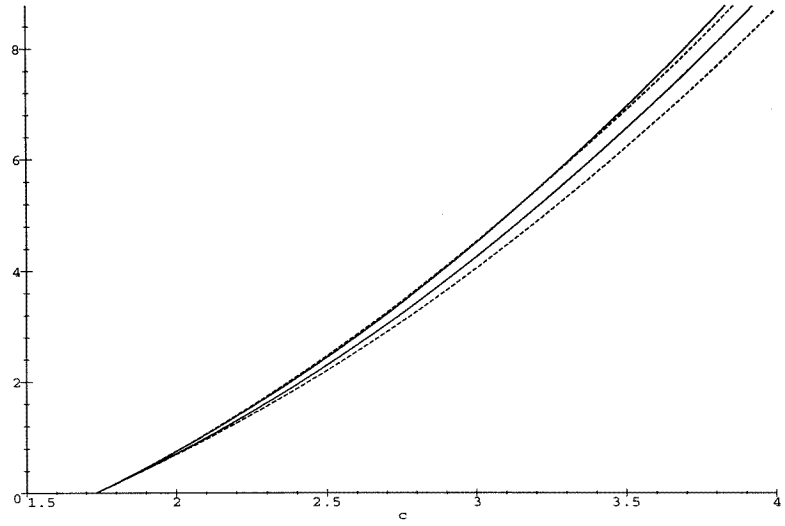

Figure 3. The figure shows height versus width curves for supersonic solitary waves in the cubic lattice with SNI, with $g = 0.5$, $a = 2$ ($b = 0$). The upper continuous line represents standard continuum approximation, the upper broken curve shows the $(2, 2)$ Padé approximate, the lower continuous line shows the Gaussian wave form from the method of identities, and the lower broken curve is the $(0, 2)$ Padé continuum approximate.

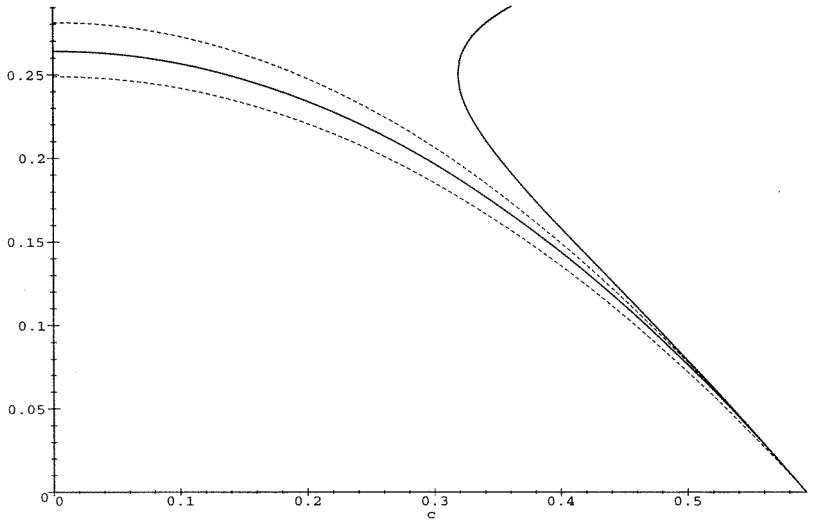

Figure 4. The figure shows height versus width curves for subsonic solitary waves in the cubic lattice with SNI, with $g = -0.162$, $a = -2$ ($b = 0$). The lower broken curve represents the Gaussian fit; the upper broken curve shows the $(2, 2)$ Padé approximation, and the full curve sandwiched between these two shows the standard continuum approximation. The other full curve which bends back on itself is from the $(0, 2)$ Padé approximation; this shows the possibility of subsonic waves ceasing to exist as the speed (c) is lowered via a saddle-node bifurcation.

5. Numerical results

First in this section we display graphs of amplitude vs speed as generated by each of the approximations in sections 3 and 4, for both supersonic and subsonic waves. These are displayed in figures 3 and 4 respectively. From these graphs we note that the speed–height characteristics for the standard continuum and $(2, 0)$ Padé continuum approximation are the same. This has already been noted indirectly earlier—the only difference between the two solutions is in the width of the wave. The differences caused by this will be seen in more detail the numerical calculations presented later in this section.

It appears that the amplitude of supersonic waves is overestimated by the standard continuum approximation, as all our other approximations lie under its height–speed curve. The $(2, 2)$ Padé lies closest to it, the $(0, 2)$ Padé gives the lowest estimate. Between these latter two lies the Gaussian waveform fitted by the method of identities. All four lines have a very similar shape.

For subsonic waves the standard continuum approximation lies between the $(2, 2)$ Padé approximate and the Gaussian fit to the identities. The $(2, 0)$ Padé method of approximation gives the same speed–height characteristics as the standard continuum approximation (as for supersonic waves) thus no separate line appears on the figure. However, the main feature from this graph comes from the $(0, 2)$ Padé approximate, which exists for a shorter range of speed values—it does not extend all the way to $c = 0$. The non-existence of slow waves in this lattice was noted by Flytzanis *et al* [12], and here we see a possible mechanism by which the existence of solutions is lost. A full numerical analysis of the bifurcation plane is needed to confirm this result, and investigate the shape of the solitary wave at its slowest speed.

From the method identities, if we assume the shape is approximately $\phi \approx A\,\mathrm{sech}^p(\beta z)$, we find that p decreases with c for subsonic waves. In the limit $p \to 0$, the shape forms a corner ($\phi \approx A\exp(-\tilde{\beta}|x|)$). Although the method of identities does not imply that p actually reaches zero for values of c we are interested in, we can speculate that slow waves cease to exist due to the formation of a cusp. This type of behaviour has been seen in other types of solitary wave equation such as the electrical lattice [9], and a nonlocal nonlinear Schrödinger equation studied by Christiansen and Rasmussen [4].

The approximations to solitary waves generated in the above two sections have been used as initial conditions in numerical integration of the lattice equations (1.2). The numerical scheme used is that of Candy and Rozmus [2]. This is a symplectic scheme for Hamiltonian systems of ODEs, and has been shown to be more accurate, efficient and easier to program than common Runge–Kutta methods [7].

Table 1. Accuracy of supersonic waves generated by the methods proposed earlier for the cubic SNI lattice with $g = \frac{1}{2}$, $a = 2$, $b = 0$.

Wave speed, c	1.8	2.0	2.5	3.0	3.5	4.0
Standard continuum	91.6% $H = 0.49$	99.7% $H = 5.04$	99.4% $H = 44$	N/A	N/A	N/A
(2, 0) Padé continuum	91.2% $H = 0.50$	99.6% $H = 5.32$	99.99% $H = 52.6$	99.86% $H = 205$	N/A	N/A
(0, 2) Padé continuum	87.7% $H = 0.54$	96.2% $H = 6.44$	96.1% $H = 68.1$	96.4% $H = 278$	N/A	N/A
Global approx to Fourier operator	78.2% $H = 0.72$	93.6% $H = 8.26$	92.4% $H = 92.2$	92.4% $H = 395$	N/A	N/A
Gaussian fitted by identities	83.1% $H = 0.58$	97.0% $H = 6.26$	98.6% $H = 61.9$	99.25% $H = 245$	99.6% $H = 707$	99.8 $H = 1696$

The calculation of the accuracy percentage is based on the proportion of the total energy in the system which is contained in the seven lattice points closest to (and including) the node with maximum amplitude. This provides an accurate measurement for fast waves which are highly localized, but underestimates the accuracy of waves very close to the continuum limit—which are spread out over many more lattice sites. However, these waves are easily approximated by any one of a variety of methods; the aim of this paper is to find methods which work well a long way from the continuum limit.

In all cases of waves away from the continuum limit, we see that the (2, 0) Padé approximation is an improvement on the standard continuum approximation. The only difference between these two is the width scale of wave—their speed–height characteristics, and shapes are identical (both being sech^2 curves in the cubic lattice and sech in the quartic case).

Away from the continuum limit we also see that supersonic waves are even better approximated by the (0, 2) and (2, 2) Padé approximates, the global approximation and the Gaussian fit. These are all new approximations for this lattice. The (2, 2) Padé method suffers from the drawback that while a speed-height relationship can be found for all relevant speeds, the waveform can only be calculated if $c^2 > 20g$. This is a limitation of the method, hence no results at all are displayed for the cubic lattice in this case.

Table 2. Accuracy of supersonic waves generated by the methods proposed earlier for the quartic SNI lattice with $g = \frac{1}{2}$, $a = 0$, $b = 2$.

Wave speed, c	1.8	2.0	2.5	3.0	3.5	4.0	100
Standard continuum	95.8% $H = 2.71$	99.88% $H = 6.56$	95.9% $H = 16.5$	81.2% $H = 31.6$	62.4% $H = 57.9$	48 % $H = 102$	33 % 5×10^8
(2, 0) Padé continuum	95.5% $H = 2.74$	99.82% $H = 6.93$	99.3% $H = 20.0$	96.6% $H = 41.6$	93.1% $H = 77.2$	89.9% $H = 132$	74 % 5.5×10^8
(0, 2) Padé continuum	91.2% $H = 3.26$	90.6% $H = 9.87$	88.8% $H = 35.0$	92.1% $H = 71.8$	98.0% $H = 108$	98.4% $H = 188$	91.8% 1.3×10^8
(2, 2) Padé continuum	N/A	N/A	N/A	N/A	95.9% $H = 78.7$	96.9% $H = 138$	98.0% 9.3×10^7
Global approx to Fourier operator	84.6% $H = 4.0$	90.3% $H = 10.8$	91.7% $H = 36.5$	92.9% $H = 84.0$	93.7% $H = 164$	94.2% $H = 288$	95.6 % 1.2×10^9
Gaussian fitted by identities	85.% $H = 3.64$	93.6% $H = 9.2$	97.0% $H = 27.5$	98.7% $H = 59.2$	99.4% $H = 111$	99.7% $H = 187$	98.9 % 6.3×10^8

Table 3. Accuracy of subsonic waves generated by the methods proposed earlier for the cubic SNI lattice with $g = -0.2$, $a = -2$, $b = 0$.

Wave speed, c	0.4	0.35	0.3
Standard continuum	88.4 % $H = 0.000\,866$	97.9 % $H = 0.001\,93$	99.6 % $H = 0.002\,65$
(2, 0) Padé continuum	88.7% $H = 0.000\,874$	99.4 % $H = 0.001\,95$	96.3 % $H = 0.002\,70$
(0, 2) Padé continuum	87.9% $H = 0.000\,856$	95.3 % $H = 0.001\,88$	97.3 % $H = 0.002\,56$
(2, 2) Padé continuum	83.2% $H = 0.000\,992$	98.6 % $H = 0.002\,44$	91.5 % $H = 0.003\,58$
Gaussian fitted by identities	83.7% $H = 0.001\,03$	92.0 % $H = 0.002\,28$	96.0 % $H = 0.003\,12$

The method based on a global approximation to the operator in Fourier space works well for the $c \to \infty$ case, where simple accurate explicit expressions are generated, but it is never as good as the (2, 2) Padé approximation or the Gaussian. All other methods give good results for the expected ranges of speed.

Fast waves in the cubic lattice are hard to generate since there is always the possibility that energy which does not form part of the soliton will cause a node to mount the potential barrier, (at $\phi = -1/a$) and drag its neighbours towards $-\infty$ with it. This is the reason that several of the entries in the table of results for the cubic lattice only contain 'N/A'. However, this demonstrates the extra accuracy gained by used the Gaussian fit or global approximation to operator.

The Gaussian waveform has very rapid decay to zero, (faster than exponential), thus gives a narrower waveform than many of the continuum approximations, and gives exceptionally accurate approximation for fast waves. This is consistent with the the results of section 2, where we saw that very fast waves ($c \to \infty$) also have rapid decay ($\phi \sim \mathrm{e}^{-\lambda z}$ with $\lambda \to \infty$).

For subsonic waves, the new methods achieve the same degree of accuracy as the standard continuum approximation. However, for fast supersonic waves, the new methods show a great improvement over the standard continuum approximation as well as the improved continuum approximation of Collins and Rice [5, 6], and are valid not just near the continuum limit, but for virtually all wave speeds.

6. Discussion

The aim of this paper has been to analyse a lattice with second-neighbour interactions (SNI). Various analytic tools have been used to extract information about the shape, height, energy and width of solitary waves supported on such a lattice. We have shown that it is possible to extend the higher order continuum methods developed in [22], to more general lattice equations; even though these methods make some use of the special structure of the equations.

In section 2 it was shown that an exact travelling wave can have a tail, which while decaying to zero, oscillates around its limiting value. The possibility of having such oscillations means that great care needs to be taken when interpreting data from numerical simulations. The development of oscillations in a tail does not necessarily imply the non-existence of an exact solitary wave.

An exact travelling wave having spatial oscillations in its tail has been studied in continuous systems previously, see Champneys and Toland [3] for example; but as far as I am aware, this is the first mention of the phenomenon in spatially discrete systems.

Several different methods of forming Continuum approximations to the solitary waves are presented in section 3. These vary in complexity, from a modification of the standard continuum approximation to the algebraically complex, but highly accurate $(2, 2)$ Padé approximate. New ideas about loss of existence of subsonic solitary waves come principally from the $(0, 2)$ Padé approximation, where the operator is applied to the nonlinear function of the waveform. This inevitably leads to more complex equations than cases where the operator acts directly on just the waveform; but in the cases studied here, we still obtain soluble equations. In the case of subsonic solitary waves, the $(2, 0)$ Padé approximation to the speed–height curves undergoes a saddle-node bifurcation, which would explain the existence of subsonic waves close to the speed of sound, but the apparent non-existence of waves with speeds close to zero. This explanation gives an approximation to a minimum speed of wave.

Such a scenario is supported to some extent by the $(2, 2)$ Padé approximant, which we would expect to be more accurate. This also predicts two branches of solutions near $c^2 = 1 + 4g$, $\phi_0 = 0$ in bifurcation space. However, the local analysis that these methods are based on do not predict the branches will meet with positive c^2 (that is this method of approximation predicts a bifurcation point outside our region of interest). Whilst the $(2, 2)$ Padé approximation is more accurate than other approximations when c^2 is near $1 + 4g$, we cannot expect quantitatively accurate answers for c^2 far away from this value. The existence (or otherwise) and position of the saddle-node bifurcation needs to be analysed using a highly accurate numerical path-following code. Numerical simulations show that the $(2, 2)$ Padé approximant is highly accurate for supersonic waves with speed much larger

than the speed of sound.

The method of identities is a novel approach to forming approximations to solitary waves. Whilst it requires some insight in finding a suitable ansatz function to use, it provides highly accurate approximations to solitary waves. The Gaussian approximation for fast supersonic waves is both accurate and easy to use, and leads to a good understanding in the differences in shape between waves near the continuum limit and those further away.

Remoissenet and Michaux [18] used a lattice equation to model electrical transmission lines. Their lattice equation supports supersonic solitons which have the same property as subsonic solitons described in this paper. That is, the shape parameter n (as defined in section 4) *decreases* as we move away from the continuum limit approximation. This represents a 'pinching' of the crest of the wave, which if taken to $n = 0$ would form a corner singularity. Such changes of shape are only identified by the method of identities, and are not detected so easily by continuum methods. A similar result has been found by Christiansen and Rasmussen [4] in a nonlocal nonlinear Schrödinger equation.

Our approximations have all been tested in a numerical integrator of the full system of ODEs, by inserting our estimates as initial conditions for the system. The amount of energy forming a solitary wave at some later time is calculated and used to calculate the accuracy of each approximation. Energy which does not form part of a solitary wave is radiated as small amplitude waves, and becomes dispersed throughout the lattice. The new approximations are seen to be significant improvements on the types of approximation commonly used in studies of solitary waves in lattices.

The methods outlined in section 3 are not easily generalized to arbitrary SNI (i.e. a general W), due to the difficulty in isolating all the explicitly k-dependent terms into a single multiplier. Diatomic lattices present more complications, since the variations in mass have to be taken into account. It is hoped to be able to extend this work to cover that case in the near future. The diatomic lattice considered by Kofane *et al* [13] has been analysed using continuum methods of higher accuracy similar to those used here [30].

Acknowledgments

I would like to thank Professor J C Eilbeck for many useful discussions, and also Professor Ostrovskii for an interesting discussion. This work was started while I was in the Department of Mathematics at Heriot–Watt University, Edinburgh, under funding from SERC. I am also grateful to the EC for funding under science programme SCI-0229-C89-100079/JU1, and to NATO for funding from the Special Programme Panel on Chaos, Order and Patterns. The latter part of this work has been aided by a grant from the Nuffield Foundation—for which I would like to express my thanks.

Appendix A.

Using the definitions $J_{m,n} \stackrel{\text{def}}{=} \frac{I_{m,n}}{I_{0,n}}$, $K_{m,n,p} \stackrel{\text{def}}{=} J_{m,n} - J_{m,np}$, the quadratic referred to in section 4 and derived from the third identity (4.2) after substituting for A and β from (4.4) is

$$\begin{aligned}[K_{4,n,p} - 6K_{2,n,p}J_{2,np} - \tfrac{12}{5}K_{2,n,p}^2]c^4 + 6[&4gK_{4,n,p} + (1-8g)K_{2,n,p}J_{2,np} \\ &-(1+16g)K_{2,n,p}J_{2,n} + \tfrac{2}{5}(1-56g)K_{2,n,p}^2]c^2 \\ &+72g[2gK_{4,n,p} + (1+4g)K_{2,n,p}J_{2,np} \\ &-(1+16g)K_{2,n,p}J_{2,n} + 2(1+4g)K_{2,n,p}^2] = 0. \end{aligned} \tag{A1}$$

Instead of regarding c as a function of n and trying to solve the above equation for n, we shall regard n as the independent variable, and investigate the effect of varying n on the other quantities. The larger root is taken, since this agrees with the continuum results in the limit $c^2 \to 1 + 4g$.

The width (4.3) remains finite in both $n \to 0, \infty$ limits

$$\text{width} \xrightarrow{n\to 0} 2p\log(2)\sqrt{\frac{(p^2-1)(c^2+12g)}{3(c^2-4g-1)}}\left(1+\frac{n}{2}\right)$$

$$\text{width} \xrightarrow{n\to\infty} \left[\frac{4p\log(2)}{3(p-1)}\left(\frac{c^2-4g-1}{c^2+12g}\right)\right]^{1/2}\left(1+\frac{(p+1)}{2np}+O(n^{-3/2})\right)$$

and in the limit $n \to 0$

$$A^{p-1} \sim p\left(\frac{c^2-4g-1}{a}\right) \qquad \beta^2 \sim \frac{12}{n^2p^2}\left(\frac{c^2-4g-1}{c^2+12g}\right)(p^2-1). \tag{A2}$$

However, it can be shown that for this particular model n will not actually reach zero for positive c^2.

References

[1] Bambusi D 1996 Exponential stability of breathers in Hamiltonian networks of weakly coupled oscillators *Nonlinearity* **9** 433–57

[2] Candy J and Rozmus W 1991 A symplectic integration algorithm for separable Hamiltonian functions *J. Comput. Phys.* **92** 230–56

[3] Champneys A R and Toland J. F 1993 Bifurcation of multi-modal homoclinic orbits for autonomous Hamiltonian systems *Nonlinearity* **6** 665–721

[4] Christiansen P L, Rasmussen K O, Johansson M, Gaididei Yu B and Bang O 1995 On some NLS systems and their applications *Proc. Euroconf. on Nonlinear Klein–Gordon and Schrödinger Systems: Theory and Applications* ed L Vazquez, L Streit, V M Perez-Garcia (Singapore: World Scientific) pp 215–33 (see particularly pp 230–32)

[5] Collins M A 1981 A quasi-continuum approximation for solitons in an atomic chain *Chem. Phys. Lett.* **72** 342–7

[6] Collins M A and Rice S A 1982 Some properties of large amplitude motion in an anharmonic chain with nearest neighbour interactions *J. Chem. Phys.* **77** 2607–22

[7] Duncan D B and Walshaw C H 1991 A symplectic solver for lattice equations *Nonlinear Coherent Structures in Physics and Biology (Lecture Notes in Physics 393)* ed M Remoissenet and M Peyrard (Berlin: Springer) pp 151–8

[8] Duncan D B and Wattis J A D 1992 Approximations to solitary waves on lattices, use of identities and the Lagrangian formulation *Chaos, Solitons and Fractals* **2** 505–18

[9] Eilbeck J C 1991 Numerical studies of solitons on lattices *Nonlinear Coherent Structures in Physics and Biology (Lecture Notes in Physics 393)* ed M Remoissenet and M Peyrard (Berlin: Springer) pp 143–50

[10] Eilbeck J C and Flesch R 1990 Calculation of families of solitary waves on discrete lattices *Phys. Lett.* A **149** 200–2

[11] Flytzanis N and Pnevmatikos S and Remoissenet M 1985 Kink, breather and asymmetric envelope or dark solitons in nonlinear chains: I monatomic chains *J. Phys. C: Solid State Phys.* **18** 4603–29

[12] Flytzanis N and Pnevmatikos S and Remoissenet M 1987 Soliton resonances in atomic nonlinear systems *Physica* **26D** 311–20

[13] Kofane T and Michaux B and Remoissenet M 1988 Theoretical and experimental studies of diatomic lattice solitons using an electrical transmission line *J. Phys. C: Solid State Phys.* **21** 1395–412

[14] Konwent H and Machnikowski P and Radosz A 1996 Dynamics of a hydrogen-bonded linear chain with a new type of one-particle potential *J. Phys.: Condens. Matter* **8** 4325–38

[15] MacKay R S and Aubry S 1994 Proof of existence of breathers for time-reversible or Hamiltonian networks of weakly coupled oscillators *Nonlinearity* **7** 1623–43

[16] Pnevmatikos S and Flytzanis N and Remoissenet M 1986 Soliton dynamics of nonlinear diatomic lattices *Phys. Rev.* B **33** 2308–21

[17] Peyrard M and Pnevmatikos S and Flytzanis N 1986 Discreteness effects on non-topological kink soliton dynamics in nonlinear lattices *Physica* **19D** 268–81
[18] Remoissenet M and Michaux B 1990 Electrical transmission lines and soliton propagation in physical systems *Proc. CMDS6 Conf. (Dij 1989)* ed G Maugin (Longman) pp 313–24
[19] Rosenau P 1986 Dynamics of nonlinear mass spring chains near the continuum limit *Phys. Lett.* **118A** 222–7
[20] Slot J J M and Janssen T 1988 Dynamics of kinks in modulated crystals *Physica* **32D** 27–71
[21] Slot J J M and Janssen T 1988 Multi-kinks in modulated crystals: the soliton lattice of the frustrated ϕ^4 model *J. Phys. A: Math. Gen.* **21** 3559–74
[22] Wattis J A D 1993 Approximations to solitary waves on lattices, II: quasi-continuum approximations for fast and slow waves *J. Phys. A: Math. Gen.* **26** 1193–209
[23] Wattis J A D 1993 Solitary waves on a two-dimensional lattice *Phys. Scr.* **50** 238–42
[24] Friesecke G and Wattis J A D 1994 Existence theorem for solitary waves on lattices *Commun. Math. Phys.* **161** 391–418
[25] Flytzanis N, Malomed B A and Wattis J A D 1993 Analysis of stability of solitons in one-dimensional lattices *Phys. Lett.* A **180** 107–12
[26] Duncan D B, Eilbeck J C, Feddersen H and Wattis J A D 1993 Solitons on lattices *Physica* **68D** 1–11
[27] Wattis J A D 1996 Continuum approximations to breather modes in generalizations of the discrete Sine–Gordon equation, in preparation
[28] Wattis J A D 1995 Variational approximations to breather modes in the discrete Sine–Gordon equation *Physica* **82D** 333–9
[29] Wattis J A D 1996 Variational approximations to breather modes in the discrete Sine–Gordon equation *Nonlinearity* **9** to appear
[30] Wattis J A D 1996 Continuum approximation to solitary waves in a diatomic lattice with nearest-neighbour and second-neighbour interactions, in preparation
[31] Woodhouse N M J 1987 *Introduction to Analytical Dynamics* (Oxford: Oxford University Press)